Received: 6 January 2020 | Revised: 9 February 2020 | Accepted: 16 February 2020

DOI: 10.1002/col.22493

WILEY

RESEARCH ARTICLE

Categorical observers for metamerism

Yuta Asano[1,2] | **Mark D. Fairchild**[1]

[1]Rochester Institute of Technology, Integrated Sciences Academy, Program of Color Science/Munsell Color Science Laboratory, Rochester, New York

[2]E Ink Corporation, Billerica, Massachusetts

Correspondence
Mark D. Fairchild, Rochester Institute of Technology, Integrated Sciences Academy, Program of Color Science/Munsell Color Science Laboratory, Rochester, NY 14623.
Email: mark.fairchild@rit.edu

Abstract

A method is proposed to generate categorical colour observer functions (individual colour matching functions) for any field size based on the CIE 2006 system of physiological observer functions. The method combines proposed categorical observer techniques of Sarkar et al with a physiologically-based individual observer model of Asano et al and a clustering technique to produce the optimal set of categorical observers. The number of required categorical observers varies depending on an application with as many as 50 required to predict individual observers' matches when a laser projector is viewed. However, 10 categorical observers are sufficient to represent colour-normal populations for personalized colour imaging. The proposed and recommended categorical observers represent a robust and inclusive technique to examine and quantify observer metamerism in any application of colorimetry.

KEYWORDS

colour matching functions, colorimetry, metamerism, observer categories, observer metamerism

1 | INTRODUCTION

A synthetic vision model for individual colorimetric observers has been proposed by Asano et al.[1] It has been used to estimate individual colour matching functions (CMFs) as well as being beneficial for simulating colour matches and identifying the range of matches among colour-normal populations. The model is an extension of the CIE 2006 physiological observers[2] (CIEPO06) and includes eight additional physiological parameters with corresponding population variability defined by standard deviations. The model can simulate CMFs that represent a population for a given age (or a given age distribution) and a field size using Monte Carlo simulation. The required steps to implement the model using Monte Carlo simulation technique are as follows:

1. Choose an age distribution and a field size as input;
2. Randomly pick age (in case an age distribution is input) and deviation values for the eight physiological parameters; and
3. Generate as many CMFs as necessary.

The model was derived with two steps; standard deviations of eight physiological parameters were obtained from past studies in the first step; the obtained standard deviations were scaled down to fit colour matching data in the second step. The final standard deviations are the current-available best estimates of interobserver variability. The model was validated using three different datasets: the Stiles-Burch colour matching data with 49 observers,[3] five-colour matches with 76 observers,[4] and Rayleigh matches with 113 observers.[5]

In this article, a set of categorical observers for use in quantification of observer metamerism potential is proposed. The idea was initiated by Sarkar,[6,7] where eight observer categories and their corresponding CMFs were proposed. Including the CIE 1964 standard observer as one observer category, Sarkar performed classified colour-normal human observers into the nine observer categories with different nominal sets of CMFs. Since categorical observers are finite and discrete, as opposed to observer functions generated from the individual colorimetric observer model, they offer a less accurate but more convenient and practical approach toward specifying observer

metamerism or creating a personalized colour imaging workflow. For example, whenever CMFs measurement or estimation is not possible, a display profile can be prepared for each categorical observer, and a viewer can pick a profile that appears most appropriate based on his/her colour vision. Additionally, due to the limited number of observer functions, categorical observers enable more convenient colour matching analyses than the Monte Carlo simulation approach using the individual observer model.

A different approach was taken from that of Sarkar.[6,7] In Sarkar's work, observer categories and their corresponding CMFs were derived in two steps. At the first step, cluster analysis was performed on Stiles and Burch individual observers and CIEPO06, which produced possible observer function candidates. At the second step, an observer function that covered Stiles and Burch individual observers under a certain colour difference criterion was sought iteratively among the possible observer function candidates. The second step was repeated until all the Stiles and Burch individual observers were covered. More detailed explanations are described in Reference 6. While this approach was valid, and Stiles and Burch observers data are perhaps the most reliable historical dataset, there are at least three limitations. The first limitation is that the number of Stiles and Burch observers is merely 49 (Sarkar used 47 of them), which makes the cluster analysis susceptible to noise. The observers were also selected for consistency and the data normalized in a fashion that minimizes observer differences. Since most of the Stiles and Burch observers performed colour matches only once (no repetition), the noise attributed to intraobserver variability would be largely present in addition to other possible noise such as potential imperfect correction of rod intrusion. The second limitation is that Sarkar's observers are inherently based on 10° field of view given that experimental constraint by Stiles and Burch. This makes Sarkar's observers difficult to extend to different field sizes. The third limitation is that Sarkar's categorization might work only in a specific condition. At the second derivation step of Sarkar's observers, a specific colour space with given sets of primaries was used. Thus, the categorization might not work as expected when viewed stimuli are different from those used in the derivation process. These three limitations are further investigated below.

The two steps to obtain categorical observers in this work are as follows:

1. Generate 10 000 sets of lms-CMFs from the individual colorimetric observer model using Monte Carlo simulation; and
2. Perform cluster analysis using a modified k-medoids method to derive categorical observers iteratively.

2 | COMPUTATIONAL APPROACH

For step one, 10 000 sets of lms-CMFs were generated using the individual colorimetric observer model[1] and Monte Carlo simulation. For the eight physiological parameters (input parameters to the model except for an age and a field size), the standard deviations were taken from Reference 1, and normal distributions were assumed. The field size was set to 2°. A field size of 2° was preferred here, given that variations in the macular pigment density were mostly measured in the fovea. An age distribution was taken from US Census 2010[8] as a probability density function for Monte Carlo simulation (shown in Figure 1). The age range was limited between 10 and 70 years-old, and the average age was 38 years-old. The limited age range was because of the interest for industrial applications, the reliability of the observer model (CIEPO06 takes ages ranging from 20 to 80), and the average age being lower than 40 year-old. Note that people in their 10's were included even though it was slightly outside the age range that CIEPO06 takes, again because of the interest for applications and the average age being lower than 40 year-old. Out of the generated 10 000 sets of lms-CMFs, 1000 of them are shown in Figure 2 for visualization purposes. All the generated lms-CMFs were area-normalized and used in the clustering process (step 2). The wavelength sampling was 5 nm from 390 to 780 nm. Thus, a set of lms-CMFs for a given observer has 237 dimensions (= 79 × 3).

At step 2, the cluster analysis using a modified *k*-medoids method was performed, and categorical observers were derived iteratively. The *k*-medoids algorithm[9] is a clustering algorithm similar to the *k*-means algorithm, one of the most popular algorithms in data mining thanks to its simplicity.[10] Both k-means and k-medoids algorithms partition a set of data points into a small number of clusters by minimizing the distance from the data points to the nearest cluster centers (centroids). The general algorithm workflows are:

1. *k* initial centroids are randomly generated among data points (the number "*k*" needs to be defined in advance);
2. *k* clusters are created by classifying all the data points to the nearest centroids;
3. For each cluster, the average of data points is computed and becomes a new centroid; and
4. The workflow 2 and 3 are repeated until convergence has been reached.

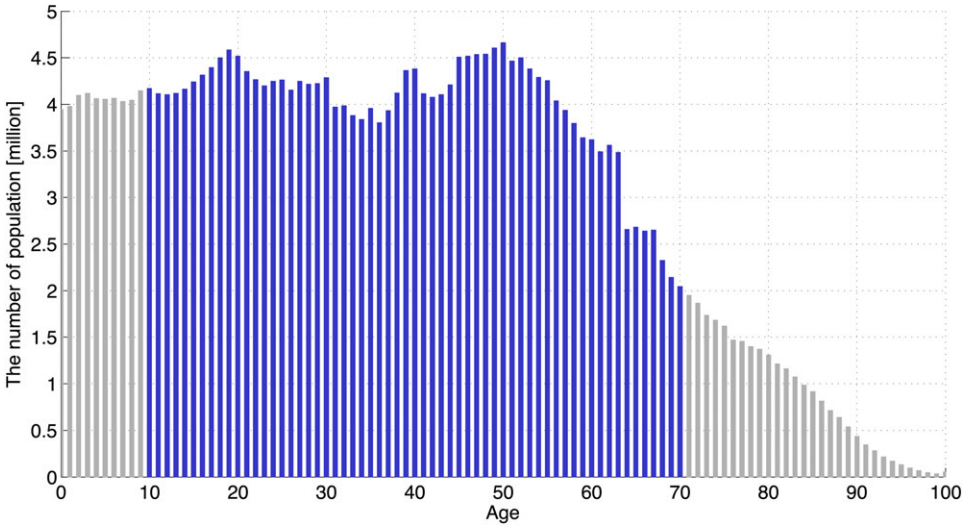

FIGURE 1 Age distributions from 2010 US Census. The age ranges used for Monte Carlo simulation are expressed as blue bars

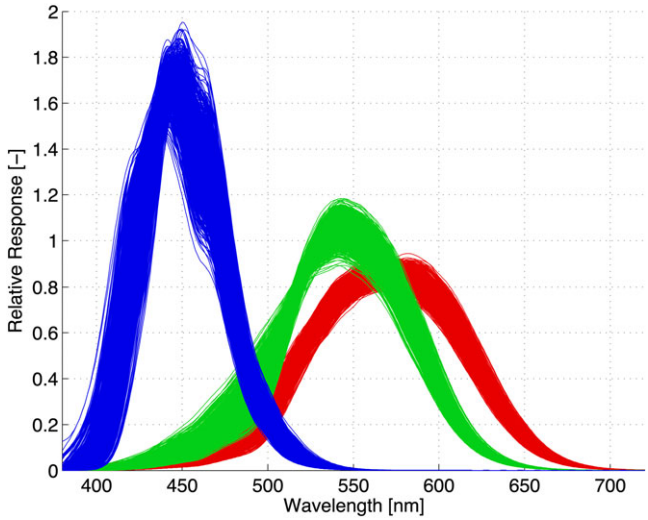

FIGURE 2 lms-CMFs (cone fundamentals) of 1000 observers generated from the individual colorimetric observer model with Monte Carlo simulation for a field size of 2°. Each function is area-normalized

The key difference between the two algorithms is that the *k*-means algorithm generates centroids that are the means of clusters whereas the *k*-medoids algorithm chooses centroids (or medoids) from data points that best represent clusters by minimizing a distance metric or a cost function. The *k*-medoids algorithm was chosen as a clustering technique in this work because the obtained centroids (or obtained categorical observers) are observer functions generated from the individual colorimetric observer model. The *k*-means algorithm outputs categorical observers whose CMFs might not happen in real human observers and merely be averages of subpopulations. Assuming the proposed individual colorimetric observer model is correct, the *k*-medoids algorithm is a more favorable approach.

The distance measure was squared Euclidean distance in cone fundamentals space. Compared with root mean squared Euclidean distance, a squared Euclidean distance puts progressively greater weight on data points that are further apart. The preliminary simulation revealed that the squared Euclidean distance produced more ideal categorical observers that cover the population.

Finally, the *k*-medoids algorithm was modified and used in this work such that each centroid (categorical observer) was derived iteratively. This iterative approach was advantageous since the number of categorical observers did not have to be specified in advance, and categorical observers could be ordered by importance in minimizing prediction error for the most observers. The modified *k*-medoids algorithm is briefly explained below.

Initially, the first centroid was fixed to the average of the 10 000 observer functions, which was an observer function with an age of 38 year-old (an average age of the population), a field size of 2°, and all the eight physiological parameters set to zero. It is equivalent to CIEPO06 function with an age of 38 year-old and a field size of 2°. No clustering process was performed to define the first centroid. Second, the number of centroids was set to two. The second centroid was a randomly picked observer function among the 10 000 functions.

The second centroid was updated (new data point was chosen) by minimizing intracluster distance measures until it reached convergence. Meanwhile, the first centroid was fixed and was not updated. The process was repeated 30 times to avoid local minima that are typical in *k*-means and *k*-medoids algorithms. Among the 30 repetitions, the data point that produced the smallest intracluster distance measure was chosen as the final, second centroid. Third, the same clustering process was performed to find the third centroid. The number of centroids was set to three, and the first and the second

centroid were fixed. Only the third centroid was updated when it reached convergence. This process was continued until 100 centroids (categorical observers) were obtained. As mentioned above, the iteratively derived categorical observers were ordered by importance. Since all the categorical observers were observers among the 10 000 sets of observer functions, the corresponding physiological parameters and ages were recorded for each categorical observer.

3 | NEW CATEGORICAL OBSERVERS

The first 10 categorical observers obtained are shown in Figure 3A. The physiological parameters and ages corresponding to the first 10 categorical observers are shown in Table 1. As noted, categorical observer 1 is the average observer among the population, thus its age is 38 years-old (average age of the population), and the eight physiological parameters were all set to zero. Categorical observer 1 is the same as CIEPO06 with age 38 year-old and a given field size. Interestingly, categorical observer 2 and 3, the second and the third most important categorical observers, have large deviations in the lens pigment density and age (both parameters control the lens and other ocular media function in the model). This implies that the variation in the lens pigment would have the most predominant effect on the overall variations in CMFs. Using the individual colorimetric observer model and the corresponding parameters from Table 1, the categorical observers can be reproduced for different field sizes. This is shown in Figure 3B for a field size of 10°. The variation of 10° CMFs is smaller than that of 2° CMFs in the short-wavelength region because the peak optical density of the macular pigment is much lower for 10° field size in comparison with 2°, which makes the absolute variation in the peak optical density of the macular pigment smaller for 10° fields. This approach follows the application across field sizes derived by Asano et al.[1]

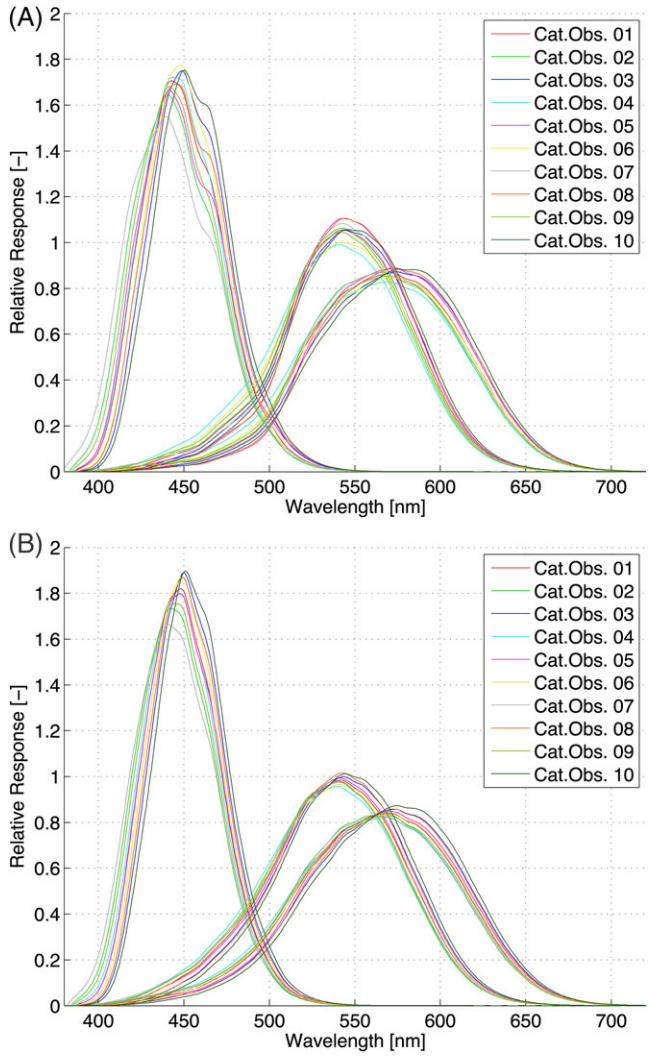

FIGURE 3 lms-CMFs (cone fundamentals) of the first 10 categorical observers for a field size of 2° (A) and 10° (B). Each function is area-normalized

The 10° categorical observers obtained in this work are compared with Sarkar's observers in Figure 4. All the CMFs were normalized such that CMFs minimized spectral RMS errors with the CIE 1964 observer. Note that Sarkar's observer category 1 was the CIE 1964 observer. The proposed categorical observers have more variations than Sarkar's observers in the short-wavelength region. The differences between the proposed categorical observers and Sarkar's observers in terms of colour matching are investigated in "Comparison with Sarkar (2011) Categorical Observers"section.

4 | PERFORMANCE

The performance of the categorical observers was evaluated by simulating colour matches for different applications. The goal of categorical observers is to reduce prediction errors in colour matches for individual human observers by having multiple observer functions instead of a single observer function. Thus, colour matches were simulated for ground-truth observer functions and categorical observer functions, and the distances (colour differences) were computed from each of the ground-truth observer matches to the nearest categorical observer matches.

To test the categorical observers with simulated colour matches, a group of metameric stimuli that might be produced in practical applications is required. In this

TABLE 1 Ages and 8 physiological parameters for the first 10 categorical observers

Categorical observers ID	1	2	3	4	5	6	7	8	9	10
Age	38	30	56	33	38	45	31	51	35	68
Lens density (%)	0	−22.9	17.0	−8.3	1.6	7.0	−34.0	15.0	−18.3	10.9
Macula density (%)	0	7.0	−11.0	−43.6	54.7	−35.3	36.3	30.8	−11.9	−16.0
Density in *L* (%)	0	−11.1	0.6	5.9	3.7	4.8	7.3	2.4	−2.4	0.7
Density in *M* (%)	0	−5.0	−5.5	4.5	16.1	11.6	7.4	−8.7	−7.0	−10.3
Density in *S* (%)	0	7.6	−1.0	0.2	−1.8	−4.5	−4.6	0.0	−9.9	9.3
Shift in *L* (nm)	0	−0.1	0.9	−1.0	1.1	−0.6	−0.6	0.5	0.3	0.7
Shift in *M* (nm)	0	0.3	0.5	−1.4	−1.1	−1.3	0.1	0.1	−0.6	0.4
Shift in *S* (nm)	0	−0.8	0.7	0.1	0.2	−0.1	0.8	0.1	−0.1	0.4

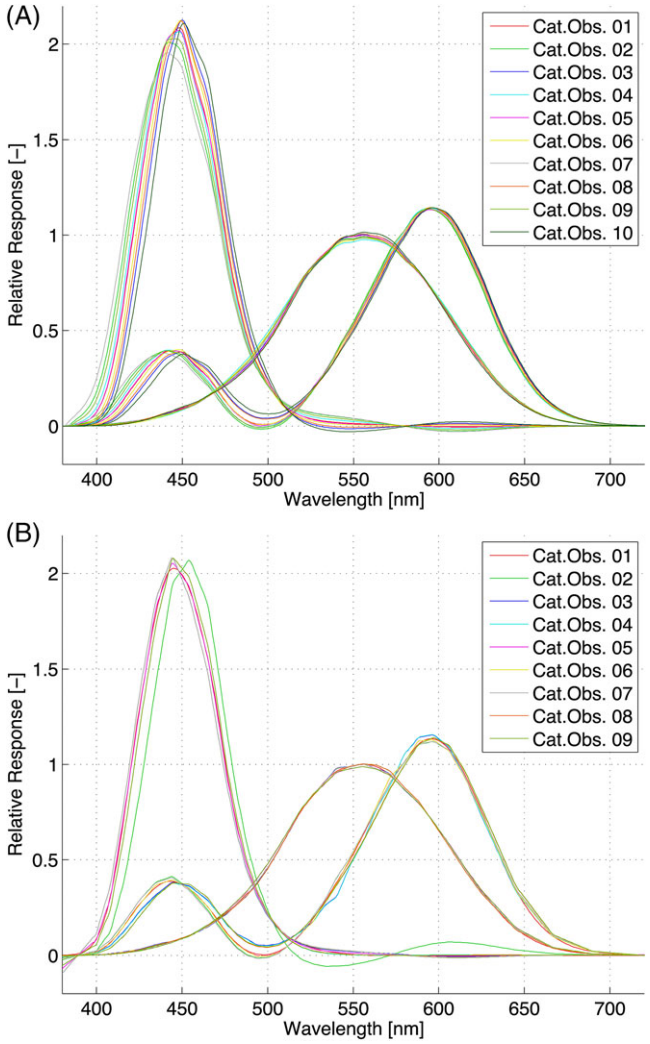

FIGURE 4 xyz-CMFs of the first 10 categorical observers for 10° (A) and xyz-CMFs of Sarkar's nine observer categories (B). All the CMFs are normalized such that CMFs minimize spectral RMS errors with the CIE 1964 observer

evaluation, metameric matches were produced for each observer and then colour differences were analyzed with a reference observer (categorical observer 1 in this case). Specifically, eight different spectral power distributions (SPD) combinations (a reference spectrum vs a set of matching primaries) were prepared from real display primaries, which would possibly be employed in soft proofing and colour grading as listed below:

1. ColorChecker white patch illuminated by D50 vs LCD with CCFL backlighting (Apple Cinema Display).
2. ColorChecker white patch illuminated by D50 vs LCD with LED backlighting (Dreamcolor LP2480zx).
3. CRT (SONY BVM32) vs LCD with CCFL backlighting (Apple Cinema Display).
4. LCD with CCFL backlighting (Apple Cinema Display) vs LCD with LED backlighting (Dreamcolor LP2480zx).
5. LCD with CCFL backlighting (Apple Cinema Display) vs OLED (Samsung Galaxy S3).
6. LCD projector (Panasonic PTAX200U) vs laser projector (Imax Laser Projector).
7. LCD with CCFL backlighting (Apple Cinema Display) vs laser projector (Imax Laser Projector).
8. Laser projector (Microvision SHOWWX+ Laser Pico Projector) vs laser projector (Imax Laser Projector).

A reference spectrum was created from a set of display primaries (SPD combination 3-8). The intensities of the display primaries were adjusted so that the chromaticity of the reference spectrum was the CIE Illuminant D50 for the CIE 1931 observer. In the other cases a ColorChecker white patch illuminated by D50 was used as a reference spectrum (SPD combination 1 and 2), the reference spectrum was obtained by multiplying the spectral reflectance of the third brightest ColorChecker neutral patch by the SPD of D50. The reference white (white point to calculate CIELAB) was assumed to have the same spectral shape as the reference spectrum with the intensity adjusted so that L^* of the reference spectrum became 65 for the CIE 1931 observer. The L^* of 65 was

meant to simulate the third brightest neutral colour match in ColorChecker 24. For observer functions, 1000 observer functions generated from the proposed individual colorimetric observer model using Monte Carlo simulation were used as ground-truth observers, and the 50 categorical observers obtained for 2° were used as categorical observers to predict ground-truth observers' matches. For each reference spectrum and matching primaries combination, exact colour matches of the 1050 observers were simulated, matched SPDs were reconstructed, and CIELAB values for the average observer (categorical observer 1, equivalent to CIEPO06 with 38 year-old and 2°) were computed. A linear transformation was performed to convert the average observer function from lms-CMFs to xyz-CMFs. The 3 × 3 matrix was estimated by a linear regression between the lms-CMFs and the CIE 1931 observer. Finally, prediction errors were computed by taking colour differences (ΔE_{00}) between CIELAB values for each ground-truth observer and CIELAB values for the nearest categorical observer. The number of categorical observers was varied between 1 and 50 to investigate the effect on prediction errors.

For SPD combination 1 (ColorChecker vs LCD with CCFL backlight), the CIELAB values for ground-truth observers and various number of categorical observers are shown in Figure 5. It shows the transition of the number of categorical observers from 2 to 5. Thanks to the iterative cluster analysis approach, the first couple of

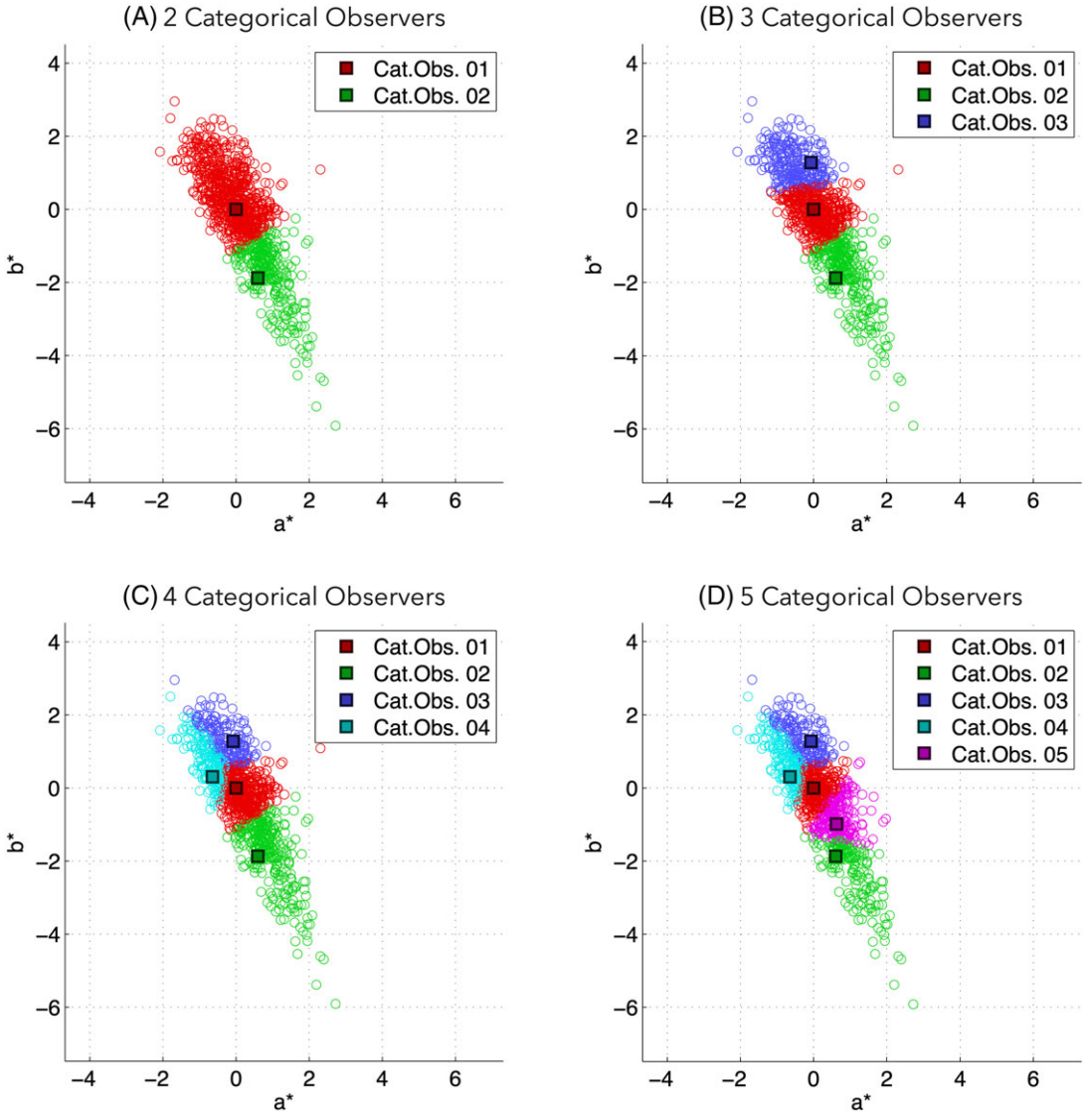

FIGURE 5 Ground-truth observers' matches (open circles) and categorical observers' matches (filled squares) plotted along CIELAB a^* and b^* axes for SPD combination 1 (ColorChecker vs LCD with CCFL backlight). Each ground-truth observer's match is colour-coded based on the nearest categorical observers. The plots are shown for different number of categorical observers (varying from 2 to 5). L^* axis is not shown because of much smaller variations

categorical observers cover the population widely, then further added categorical observers provide finer categorizations.

The average prediction errors are plotted as a function of the number of categorical observers in Figure 6. The prediction errors decrease as the number of categorical observers increases for all SPD combinations. However, the contribution from the number of categorical observers to the prediction improvement decreases progressively. Another important insight is that the required number of categorical observers highly depends on SPD combinations. For example, to achieve an average prediction error below ΔE_{00} of 1, only two categorical observers are required for ColorChecker vs LCD with CCFL (SPD combination 1, red line in Figure 6) while approximately 50 categorical observers are required for LCD with CCFL vs laser projector (SPD combination 7, gray line in Figure 6). This is quite inconvenient since there is no optimal number (within reasonably manageable numbers) of categorical observers that satisfies a certain criterion in all the applications. Nevertheless, for general use and convenience, the global number of categorical observers that could be used in any applications was sought.

The changes in average prediction errors are illustrated in Figure 7. Figure 7 indicates how much error can be decreased by adding another categorical observer. Generally, there are significant contributions having three categorical observers, small but meaningful changes (ΔE_{00} of approximately 0.1-0.2) up to 10 categorical observers, and the changes become quite small (less than ΔE_{00} of 0.1) afterwards. Another way to investigate the prediction error decrease is to normalize prediction errors by the maximum for each SPD combination as shown in Figure 8. In general, average prediction error decreases to one-third using 10 categorical observers compared to using a single observer. Given that the prediction error improvement is small after 10 observers, the prediction errors become one-third on average by introducing 10 observers, and 10 is still a manageable number, 10 categorical observers would be good for general use

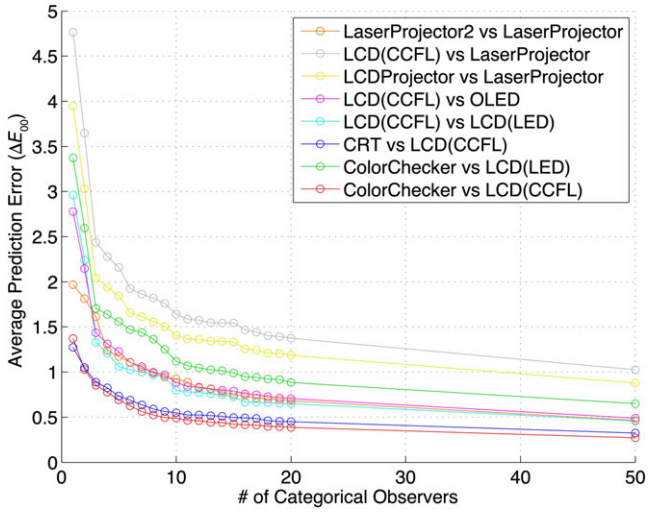

FIGURE 6 Average prediction errors (ΔE_{00}) as a function of the number of categorical observers for different SPD combinations. ΔE_{00} is taken between each ground-truth observer match and the nearest categorical observer match

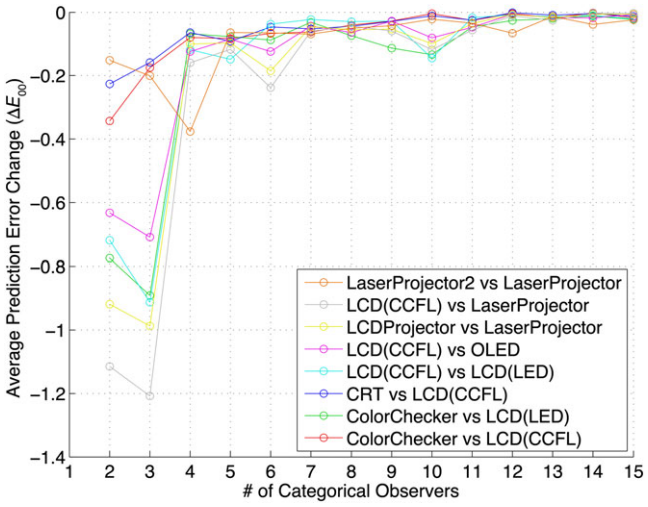

FIGURE 7 Changes in average prediction errors. For a given number of categorical observers, "k", the error change was computed between "k" and "'$k-1$" categorical observers

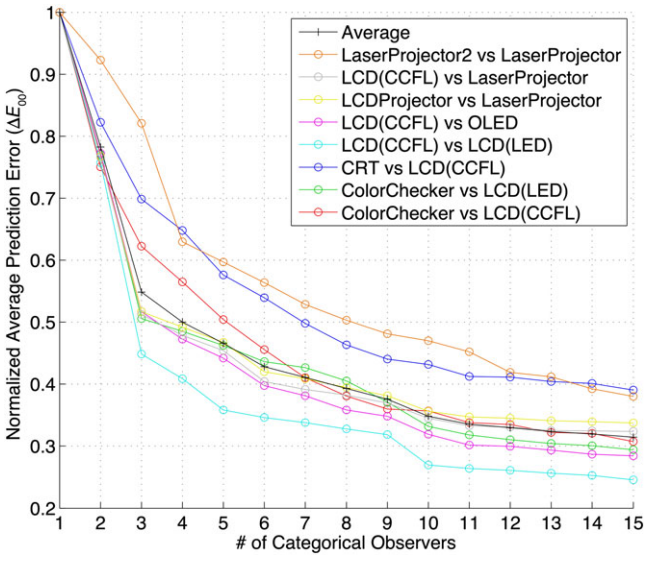

FIGURE 8 Normalized average prediction errors (ΔE_{00}) as a function of the number of categorical observers for different SPD combinations. Prediction errors are normalized by the maximum for each SPD combination. The average of the eight lines is shown as a black line with plus marks

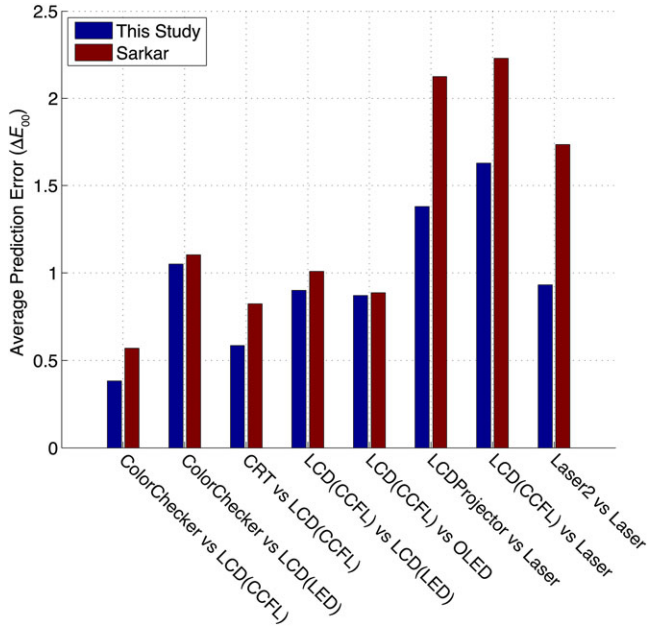

FIGURE 9 Average prediction errors of the eight different SPD combinations for the proposed, first nine categorical observers and the Sarkar nine observers. Ground-truth observers are 1000 observer functions generated from the individual colorimetric observer model with Monte Carlo simulation

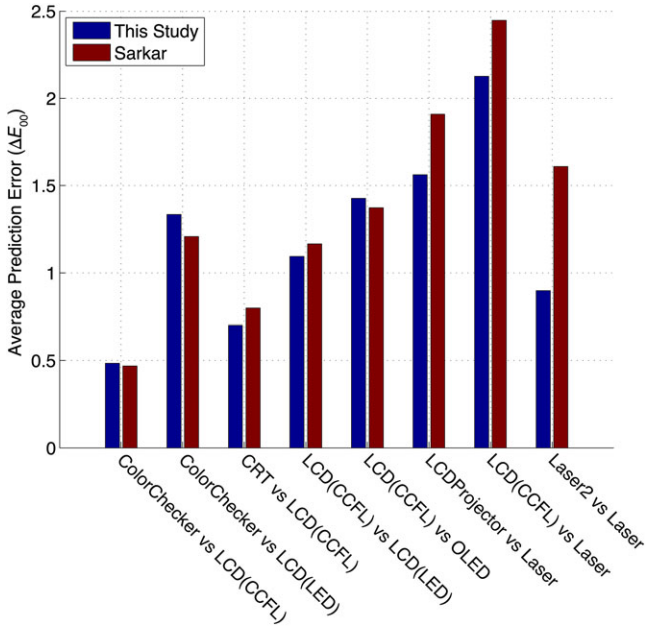

FIGURE 10 Average prediction errors of the eight different SPD combinations for the proposed, first nine categorical observers and the Sarkar nine observers. Ground-truth observers are Stiles and Burch 49 observers

and convenience to represent colour-normal populations and to be used for personalized colour imaging.

5 | COMPARISON WITH SARKAR (2011) CATEGORICAL OBSERVERS

The proposed categorical observers were then compared with Sarkar's observers[6,7] by simulating colour matches. The same simulations as those discussed above were performed. That is, categorical observers were set to either the proposed categorical observers or Sarkar's observers, then prediction errors were computed between each ground-truth observer's match and the nearest categorical observer's match. To perform a fair comparison, the field size was set to 10° and the first nine categorical observers were used for the proposed categorical observers. The comparison results are shown in Figure 9. In all the eight SPD combinations, the proposed categorical observers performed better than Sarkar's observers. For SPD combinations involving laser projectors, the improvements were more significant. Note that Sarkar's observers were derived from Stiles and Burch observers. To investigate the effect of the ground-truth observers, Stiles and Burch 49 observers were used as ground-truth observers instead of the 1000 observer functions from Monte Carlo simulation. The results are shown in Figure 10. In this case, the performance of the proposed categorical observers and Sarkar's observers is comparable. However, the proposed categorical observers still gave smaller prediction errors in cases where laser projectors were used. More detailed comparisons for SPD combination 8 (laser projector 2 vs laser projector) are shown in Figure 11.

The relative performance of Sarkar's observers can be attributed to the first limitation (susceptibility to noise) and the third limitation (optimized for a specific colour space) in that approach. The spectral integrations occur in very narrow ranges for laser primaries, which are more susceptible to noise in CMFs. Sarkar's observers might behave poorly (eg, observer category 2 in Figure 11C,D) for laser projectors since the spectral emissions are significantly different from those used in Sarkar's derivation process.

Compared with Sarkar's observers, the proposed categorical observers have the flexibility to change field size and the number of categories, they are more robust to changes in spectral combinations for the use of different applications, and they are based on CIEPO06.

6 | CONCLUSIONS

Categorical observers are a set of observer functions that would represent colour-normal populations. They are finite and discrete as opposed to observer functions

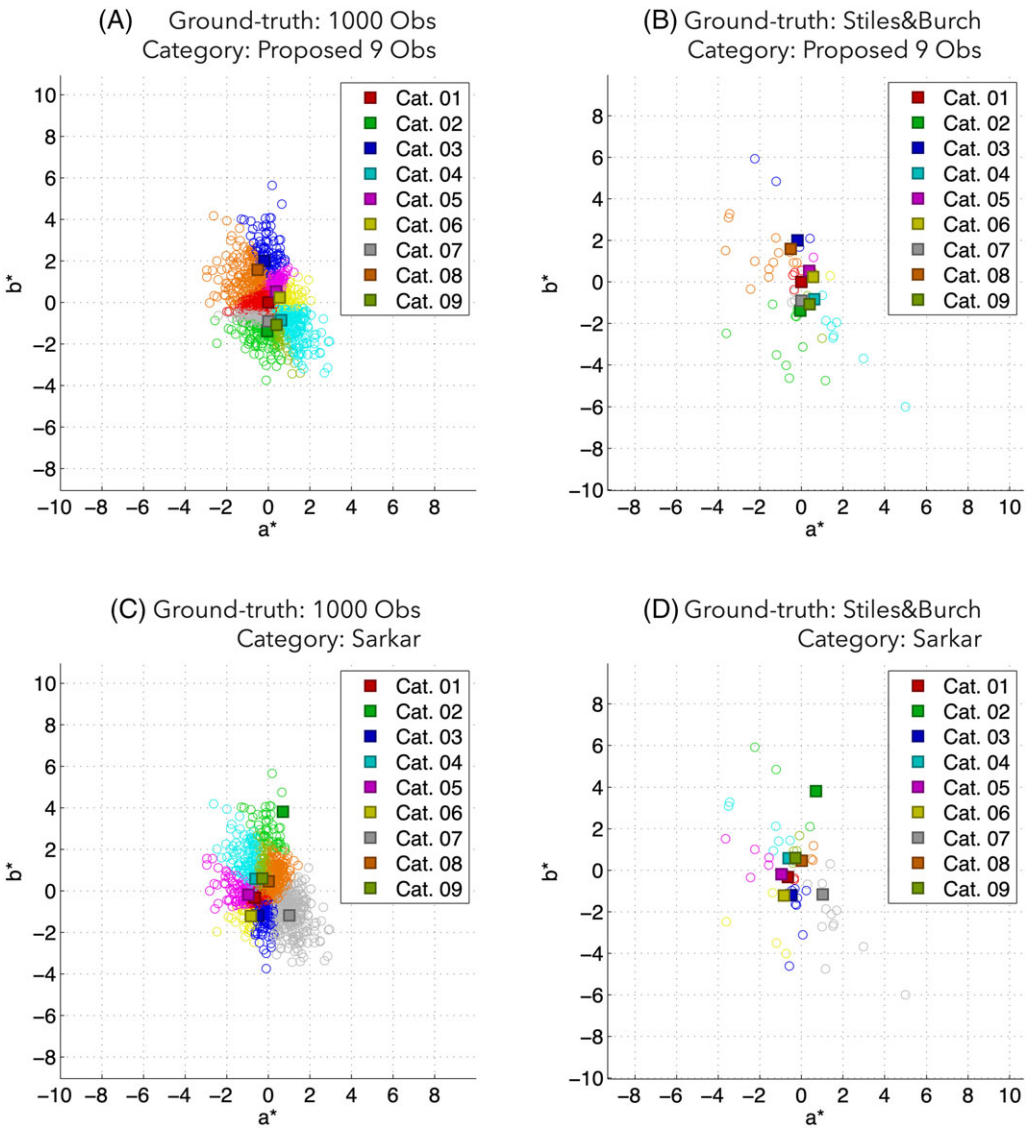

FIGURE 11 Ground-truth observer matches (open circles) and categorical observer matches (filled squares) plotted along CIELAB a^* and b^* axes for SPD combination 8 (laser projector 2 vs laser projector). Each ground-truth observer match is colour-coded based on the nearest categorical observer. Four different ground-truth and categorical observer combinations are shown. Ground-truth observers are either 1000 observers from Monte Carlo simulation or 49 Stiles and Burch observers. Categorical observers are either the proposed first nine categorical observers or the Sarkar observers

generated from the individual colorimetric observer model. Thus, they would offer more convenient and practical approaches for the personalized colour imaging workflow and any colour matching analyses. Categorical observers were derived in two steps. At the first step, 10 000 observer functions were generated from the individual colorimetric observer model using Monte Carlo simulation. At the second step, the cluster analysis, a modified k-medoids algorithm, was applied to the 10 000 observers, and 100 categorical observers were derived iteratively. Since the proposed categorical observers are defined by their physiological parameters and ages, they can be derived for any target field size. Categorical observers were ordered by the importance; the first categorical observer was the average observer equivalent to CIEPO06 with 38 year-old for a given field size, followed by the second most important categorical observers, and so on.

The number of required categorical observers varies depending on an application. For example, as many as 50 categorical observers would be required to predict individual observers' matches satisfactorily when a laser projector is viewed. The colour matching analyses showed that 10 categorical observers are good for

general use and convenience to represent colour-normal populations and to be used for personalized colour imaging. On average, the prediction error improvement was small after adding 10th categorical observers, and the prediction errors became one-third by introducing 10 observers. Comparing with Sarkar's observer categories, the proposed categorical observers generally gave better results in simulated colour matches. The significant improvements were obtained when laser projector primaries were used, due to the robustness of the proposed categorical observers against SPD combinations. In recent years, diverse display technologies such as OLEDs, LEDs, lasers, and quantum dots[11] have been emerging in the market, and spectral emissions of display primaries could be in any shape in the near future. Thus, the robustness against different spectral shapes is a key attribute for categorical observers that the present technique has attempted to anticipate to the degree possible.

ACKNOWLEDGMENTS

This research was carried out as part of the first author's PhD dissertation at the Rochester Institute of Technology, which was supported, in part, by Technicolor Research and Innovation, Rennes, France. Example colour matching functions for the categorical observers can be found online at <https://www.rit.edu/science/mcsl-research#student-research> under “Observer Function Database”.

ORCID

Mark D. Fairchild https://orcid.org/0000-0003-1848-3429

REFERENCES

[1] Asano Y, Fairchild MD, Blondé L. Individual colorimetric observer model. *PLoS One*. 2016;11(2):e0145671.

[2] CIE. *Fundamental Chromaticity Diagram with Physiological Axes—Part 1*. CIE Publication No. 170; 2006.

[3] Stiles WS, Burch JM. Interim report to the commission Internationale de l'Eclairage, Zurich, 1955, on the National Physical Laboratory's investigation of colour-matching (1955). *J Mod Opt*. 1955;2(4):168-181.

[4] Asano Y, Fairchild MD, Blondé L, Morvan P. Multiple color matches to estimate human color vision sensitivities. *Image and Signal Processing*. Springer, London; 2014:18-25.

[5] Rüfer F, Sauter B, Klettner A, Göbel K, Flammer J. Age-corrected reference values for the Heidelberg multi-color anomaloscope. *Graefes Arch Clin Exp Ophthalmol*. 2012;250 (9):1267-1273.

[6] Sarkar, A. *Identification and Assignment of Colorimetric Observer Categories and Their Applications in Color and Vision Sciences* [PhD thesis]. Université de Nantes; 2011.

[7] Sarkar A, Blondé L, Le Callet P, et al. Toward reducing observer metamerism in industrial applications: colorimetric observer categories and observer classification. *IS&T/SID Color and Imaging Conference*; Society for Imaging Science and Technology, San Antonio. 2010:307-313.

[8] US Census Bureau. *Census 2010, Summary File 1*. Table PCT12; 2010.

[9] Kaufman L, Rousseeuw P. Clustering by means of medoids. *Statistical Data Analysis Based on the L1–Norm and Related Methods*. North-Holland, Amsterdam; 1987:405-416.

[10] Wu X, Kumar V, Quinlan JR, Ghosh J, Yang Q. Top 10 algorithms in data mining. *Knowl Inform Syst*. 2008;14(1):1-37.

[11] Bourzac K. Quantum dots go on display. *Nature*. 2013;493 (7432):283.

AUTHOR BIOGRAPHIES

Yuta Asano is a Senior Image Scientist at E Ink Corporation. He received a BE in architecture and an ME in architectural engineering from Kyoto University, and a PhD in color science from Rochester Institute of Technology.

Mark D. Fairchild is Professor and Founding Head of the Integrated Sciences Academy in RIT's College of Science and Director of the Program of Color Science and Munsell Color Science Laboratory. He received BS and MS degrees in imaging science from RIT and a PhD in vision science from the University of Rochester. Mark was presented with the 1995 Bartleson Award by the Colour Group (Great Britain) and the 2002 Macbeth and 2018 Nickerson Awards by the Inter-Society Color Council (ISCC) for his works in colour appearance and colour science and contributions to the field. He is a Fellow of the Society for Imaging Science and Technology (IS&T) and the Optical Society of America (OSA). Mark was presented with the Davies Medal by the Royal Photographic Society for contributions to photography. He received the 2008 IS&T Raymond C. Bowman award for excellence in education.

How to cite this article: Asano Y, Fairchild MD. Categorical observers for metamerism. *Color Res Appl*. 2020;1–10. https://doi.org/10.1002/col.22493